

Towards Quantum Superposition of Living Organisms

Oriol Romero-Isart¹, Mathieu L. Juan², Romain Quidant^{2,3}, and J. Ignacio Cirac¹

¹Max-Planck-Institut für Quantenoptik, Hans-Kopfermann-Strasse 1, D-85748, Garching, Germany.

²ICFO-Institut de Ciències Fotoniques, Mediterranean Technology Park, Castelldefels, Barcelona, 08860 Spain and

³Institució Catalana de Recerca i Estudis Avançats, E-08010, Barcelona, Spain

The most striking feature of quantum mechanics is the existence of superposition states, where an object appears to be in different situations at the same time. The existence of such states has been tested with small objects, like atoms, ions, electrons and photons [1], and even with molecules [2]. More recently, it has been possible to create superpositions of collections of photons [3], atoms [4], or Cooper pairs [5]. Current progress in optomechanical systems may soon allow us to create superpositions of even larger objects, like micro-sized mirrors or cantilevers [6, 7, 8, 9], and thus to test quantum mechanical phenomena at larger scales. Here we propose a method to cool down and create quantum superpositions of the motion of sub-wavelength, arbitrarily shaped dielectric objects trapped inside a high-finesse cavity at a very low pressure. Our method is ideally suited for the smallest living organisms, such as viruses, which survive under low vacuum pressures [10], and optically behave as dielectric objects [11]. This opens up the possibility of testing the quantum nature of living organisms by creating quantum superposition states in very much the same spirit as the original Schrödinger’s cat “gedanken” paradigm [12]. We anticipate our essay to be a starting point to experimentally address fundamental questions, such as the role of life and consciousness in quantum mechanics.

The ultimate goal of quantum optomechanics is to push the motion of macroscopic objects towards the quantum limit, and it is a subject of interest of both fundamental and applied science [7, 8, 9]. The typical experimental setup consists of an optical cavity whose resonance frequency depends on the displacement of some mechanical oscillator. The mechanical motion shifts the resonance frequency, and, consequently, the radiation pressure exerted into the mechanical object. The overall effect yields the optomechanical coupling which should enable us to cool down to the ground state the mechanical motion [13, 14, 15]. We are currently witnessing an experimental race to reach the ground state using different setups, such as, nano- or microcantilevers [16], membranes [17], or vibrating microtoroids [18]. It is expected that the achievement of the ground state will open up the possibility to perform fundamental and applied experiments involving quantum phenomena with these macroscopic objects, as pioneered by the work of Marshall *et al* [6].

In this Letter, we propose dielectric objects levitating inside the cavity as new quantum optomechanical systems. The fact that those are not attached to other mechanical objects avoids the main source of heating, which is present in other optomechanical systems, and thus, should facilitate the achievement of ground state cooling. Once this is achieved, we propose to create quantum superpositions of the center of mass motional state of the object by sending a light pulse to the cavity simultaneously pumped with a strong field, and a subsequent detection of the reflected light field. One of the main features of this proposal is that it applies to a wide variety of new objects and, in particular, to certain living organisms. Therefore, our proposal paves the path for the experimental test of the superposition principle with living creatures.

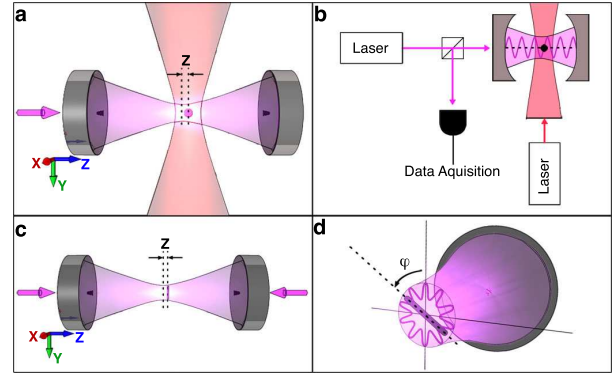


Fig. 1: **Quantum optomechanics with dielectric objects trapped inside a high-finesse optical cavity.** a) A dielectric sphere is trapped by optical tweezers inside a high-finesse optical cavity. The confinement of the center-of-mass motion along the z -axis is harmonic with frequency ω_t . The driving field generates a radiation pressure able to cool down the mechanical motion to the ground state. b) Experimental setup for trapping and cooling of dielectric spheres using two lasers, one for the driving and one for the trapping. c) The center-of-mass motion of a dielectric rod can also be trapped and cooled. In this case we assume self-trapping achieved by using two laser modes, see appendix C & D. d) The rotational motion of a dielectric rod can also be cooled by generating a standing wave in the azimuthal angle. This can be achieved by superimposing two counterrotating Laguerre-Gauss modes.

We consider an object with mass M , volume V , and relative dielectric constant $\epsilon_r \neq 1$, which may be non-homogeneous. The object is trapped inside a cavity, either by an external trap, provided, for instance, by optical tweezers [19] (Fig. 1a), or by self-trapping using two cavity modes (see appendix C for details). The trap is harmonic, so that the center of mass effectively

decouples from any relative degree of freedom. Along the cavity axis, this requires the size of the object to be smaller than the optical wavelength which is used for trapping and cooling. The center-of-mass displacement, z , is then quantized as $\hat{z} = z_m(\hat{b}^\dagger + \hat{b})$, where $\hat{b}^\dagger(\hat{b})$ are creation(annihilation) phonon operators, and $z_m = (\hbar/2M\omega_t)^{1/2}$ is the ground state size, with ω_t the trap frequency. The resonance frequency of the optical cavity ω_c^0 is modified by the presence of the dielectric object inside the cavity. A crucial relation is the frequency dependence on the position of the dielectric object, which can be computed using perturbation theory (see appendix A). This position dependence gives rise to the typical quantum optomechanical coupling,

$$\hat{H}_{\text{OM}} = g(\hat{b}^\dagger + \hat{b})(\hat{a}^\dagger + \hat{a}). \quad (1)$$

Here, $\hat{a}^\dagger(\hat{a})$ are the operators that create(annihilate) a resonant photon in the cavity. The quantum optomechanical coupling g can be written as $g = \sqrt{n_{\text{ph}}}g_0$, where n_{ph} is the number of photons inside the cavity and $g_0 = z_m\xi_0$ (ξ_0 comes from the resonance frequency dependence on the position, see appendix D). The enhancement of g_0 by a factor of $\sqrt{n_{\text{ph}}}$ has been experimentally used to achieve the strong coupling regime in recent experiments with cantilevers [20]. Finally, the total Hamiltonian also includes the mechanical and radiation energy term as well as the driving of the cavity. See appendix B for the details of these terms as well as the derivation of (1).

Besides the coherent dynamics given by the total Hamiltonian, there exists also a dissipative part provided by the losses of photons inside the cavity, parametrized by the decaying rate κ , and the heating to the motion of the dielectric object. Remarkably, our objects are trapped without linking the object to other mechanical pieces, and hence thermal transfer does not contribute to the mechanical damping γ . This fact constitutes a distinctive feature of our proposal, possibly yielding extremely high mechanical quality factors. Indeed, the most relevant source of motional heating in our scheme is the pressure inside the vacuum chamber since, as mentioned above, coupling to other modes within the object is negligible when having a quadratic potential. In appendix E, we derive that the maximum pressure required for ground state cooling is $\sim 10^{-6}$ Torr, which actually corresponds to the typical one used in optomechanical experiments [17]. The mechanical quality factor of our objects under this pressure is $\sim 10^9$, and it can be even increased in a higher vacuum. Moreover, the bulk temperature of the object remains close to the room temperature for sufficiently transparent objects at the optical wavelength, a fact that prevents its damage (see appendix F).

The rotational cooling of cylindrical objects, such as rods (see Fig. 1c), can also be considered. In this case, two counter-rotating Laguerre-Gauss modes can be employed to create a standing wave in the azimuthal angle ϕ , as illustrated in Fig. 1d. The optomechanical coupling is

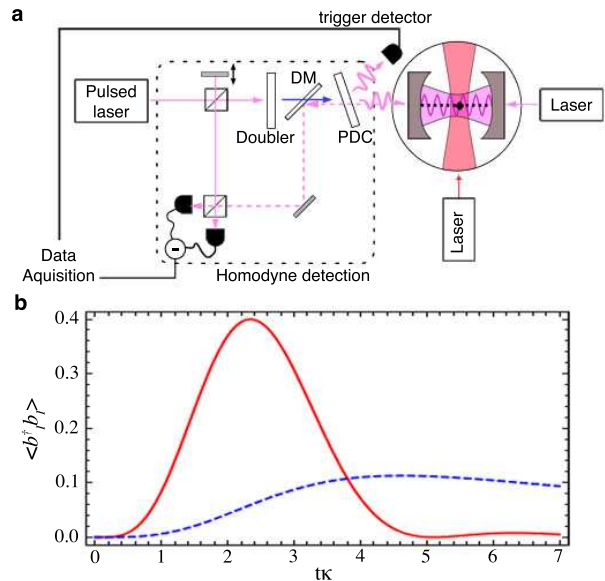


Fig. 2: **Protocol to prepare quantum superposition states.** a) Experimental setup for implementing the protocol to prepare the quantum superposition state (2). In the figure PDC stands for Parametric Down Conversion, and DM for Dichroic Mirror. A blue photon is converted into two red photons in the PDC. One is detected and the other impinges to the cavity. If it is reflected, the one photon pulse on top of the driving field goes back through the PDC (which is transparent), then reflected downwards towards the homodyne detector by the DM. b) Mean number of phonons $\langle \hat{b}^\dagger \hat{b} \rangle$ imprinted to the mechanical oscillator by sending a one photon pulse to the cavity, see appendix G for details. A gaussian pulse of width $\sigma = \kappa$ is used. The red solid line corresponds to the strong coupling regime $g = \kappa$, whereas the blue dashed one corresponds to the weak coupling $g/\kappa = 1/4$. In the strong coupling regime, the balanced homodyne measurement should be performed around the time where the mean number of phonons is maximum. This results in the preparation of the quantum superposition state (2).

then given by $g_0 = (\hbar/2I\omega_t)\xi_0$, where I is the moment of inertia. Using two modes, one can self-trap both the rotational and the center-of-mass translational motion, and cool either degree of freedom by slightly varying the configuration of the two modes (see appendix D for further details). Both degrees of motion can be simultaneously cooled if the trapping is provided externally (see Ref. [21] for a proposal to cool the rotational motion of a mirror).

Regarding the feasibility of our scheme, we require the good cavity regime $\omega_t > \kappa$, in order to accomplish ground state cooling [13, 14, 15]. Moreover, the strong coupling regime $g \gtrsim \kappa, \gamma$, is also required for quantum states generation. Both regimes can be attained with realistic experimental parameters using dielectric spheres and rods, as shown in appendix H.

We tackle now the intriguing possibility to observe quantum phenomena with macroscopic objects. Notably, the

optomechanical coupling (1) is of the same nature as the typical light-matter interface Hamiltonian in atomic ensembles [4]. Hence, the same techniques can be applied to generate entanglement between gaussian states of different dielectric objects.

A more challenging step is the preparation of non-gaussian states, such as the paradigmatic quantum superposition state

$$|\Psi\rangle = \frac{1}{\sqrt{2}}(|0\rangle + |1\rangle). \quad (2)$$

Here $|0\rangle$ ($|1\rangle$) is the ground state (first excited state) of the quantum harmonic oscillator. In the following, we sketch a protocol to create the state (2) —see appendix G for further details. The pivotal idea is to impinge the cavity with a single-photon state, as a result of parametric down conversion followed by a detection of a single photon [22]. When impinging into the cavity, part of the field will be reflected and part transmitted [23]. In the presence of the red-detuned laser, the coupling (1) swaps the state of light inside the cavity to the mechanical motional state, yielding the entangled state $|E\rangle_{ab} \sim |\tilde{0}\rangle_a|1\rangle_b + |\tilde{1}\rangle_a|0\rangle_b$. Here $a(b)$ stands for the reflected cavity field(mechanical motion) system, and $|\tilde{0}(\tilde{1})\rangle_a$ is a displaced vacuum(one photon) light state out of the cavity. The protocol ends by performing a balanced homodyne measurement and by switching off the driving field. The motional state collapses into the superposition state $|\Psi\rangle = c_0|0\rangle + c_1|1\rangle$, where the coefficients $c_{0(1)}$ depend on the measurement result. See Fig. 2 for the experimental setup and results derived in appendix G. This state can be detected by either transferring it back to a new driving field, and then performing tomography on the output field, or by monitoring the quantum mechanical oscillation caused by the harmonic trap. Moreover, the amplitude of the oscillation can be amplified by driving a blue-detuned field tuned to the upper motional sideband. Note that a loss of coherence due to “which-path” information is negligible at room and even much higher temperatures [2].

A possible extension of the protocol is to impinge the cavity with other non-gaussian states, such as the NOON state or the Schrödinger’s cat state $|\alpha\rangle + |-\alpha\rangle$ [24], where $|\alpha\rangle$ is a coherent state with phase α , in order to create other quantum superposition states. Furthermore, one can change dynamically the laser intensity to obtain a better transmission. Alternatively, one can tune the laser intensity to the upper motional sideband and detect the output light in order to relax the strong coupling condition (O.R.I. *et al.*, in preparation).

In the following we analyze the possibility of performing the proposed experiment with living organisms. The viability of this perspective is supported by the following reasons: i) living microorganisms behave as dielectric objects, as shown in optical manipulation experiments in liquids [11]; ii) some microorganisms exhibit very high

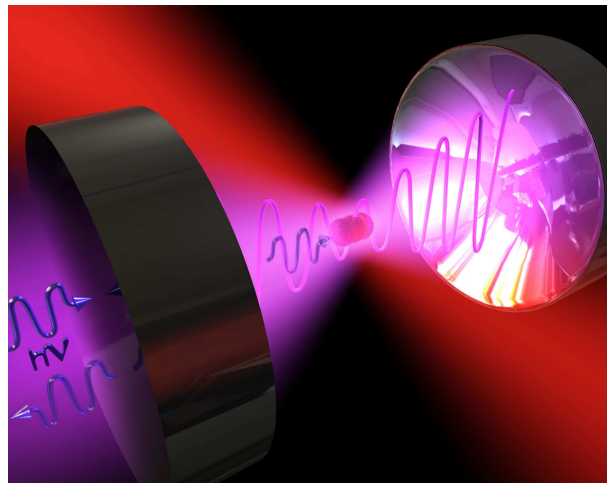


Fig. 3: **Quantum superposition of living organisms.** Illustration of the protocol to create quantum superposition states applied to living organisms, such as viruses, trapped in a high-finesse optical cavity by optical tweezers.

resistance to extreme conditions, and, in particular, to the vacuum required in quantum optomechanical experiments [10]; iii) the size of some of the smallest living organisms, such as spores and viruses, is comparable to the laser wavelength, as required in the theoretical framework presented in this work; and iv) some of them present a transparency window (which prevents the damage caused by laser’s heating), and still have sufficiently high refractive index. As an example, the common influenza viruses, with size of ~ 100 nm, can be stored for several weeks in vacuum down to 10^{-4} Torr [25]. In higher vacuum, up to 10^{-6} Torr, a good viability can be foreseen for optomechanics experiments. Due to their structure (*e.g.* lipid bilayer, nucleocapsid protein, and DNA), viruses present a transparency window at the optical wavelength which yields relatively low bulk temperatures [26]. Note that self-trapping or, alternative trapping methods, such as magnetic traps, could be used in order to employ lower laser powers. The Tobacco Mosaic Virus (TMV) also presents a very good resistance to high vacuum [10], and has a rod-like appearance of 50 nm wide and almost $1 \mu\text{m}$ long. Therefore, it constitutes the perfect living candidate for the rotational cooling, see Fig. 1d.

In conclusion, we have presented results that open the possibility to observe genuine quantum effects, such as the creation of quantum superposition states, with nanodielectric objects and, in particular, with living organisms such as viruses, see Fig. 3. This entails the possibility to test quantum mechanics, not only with macroscopic objects, but also with living organisms. A direction to be explored is the extension to objects larger than the wavelength (O.R.I. *et al.*, in preparation). This would permit to bring larger and more complex living organisms to the quantum realm; for instance, the Tardigrade, which have

a size ranging from $100 \mu\text{m} \sim 1.5 \text{ mm}$ [27], and is known to survive during several days in open space [28]. We expect the proposed experiments to be a first step to experimentally address fundamental questions, such as the role of life and consciousness in quantum mechanics, and maybe even implications in our interpretations of quantum mechanics [29].

We thank M. D. Lukin for discussions. We acknowledge funding by the Alexander von Humboldt foundation (O.R.I.), European project SCALA, the DFG –FOR635 and the excellence cluster Munich Advanced Photonics–, Spanish Ministry of Sciences through Grants TEC2007-60186/MIC and CSD2007-046-NanoLight.es, Fundació CELLEX Barcelona, and Caixa Manresa.

Note added: We also have become aware of a recent, similar proposal to optically levitate and manipulate a nano-mechanical system by D. E. Chang *et al.*, in arXiv:0909.1548.

APPENDIX A: RESONANCE FREQUENCY DEPENDENCE ON MECHANICAL POSITION

Here we show how to compute the frequency dependence on the mechanical coordinates of arbitrarily shaped dielectric objects. Note that the resonance frequency ω_c^0 , and the optical mode $\varphi_0(\vec{r})$ of the cavity without the dielectric object, are known solutions of the Helmholtz equation. The presence of the dielectric object, which is small compared to the cavity length, can be considered as a tiny perturbation on the whole dielectric present inside the cavity, and, thus, a perturbation theory can be used to obtain the resonance frequency

$$\omega_c(q) \approx \omega_c^0 \left(1 - \frac{\int_{V(q)} (\epsilon_r - 1) |\varphi_0(\vec{r})|^2 d\vec{r}}{2 \int |\varphi_0(\vec{r})|^2 d\vec{r}} \right). \quad (\text{A1})$$

Here ϵ_r is the relative dielectric constant of the object, and $V(q)$ is its volume at coordinates q . The integral in the numerator, which is performed through the volume of the object placed at coordinates q , yields the frequency dependence on q .

APPENDIX B: TOTAL HAMILTONIAN IN QUANTUM OPTOMECHANICS

The total Hamiltonian in quantum optomechanics can be typically written as

$$\hat{H}_t = \hat{H}_m + \hat{H}_r + \hat{H}_{\text{OM}} + \hat{H}_{\text{drive}}. \quad (\text{B1})$$

The term H_m corresponds to the mechanical energy of the degree of motion $\hat{q} = q_m(\hat{b}^\dagger + \hat{b})$, which is assumed to be harmonically trapped. Therefore, $\hat{H}_m = \hbar\omega_t \hat{b}^\dagger \hat{b}$,

where ω_t is the trapping frequency. The driving of the cavity field, with a laser at frequency ω_L and strength E , related to the laser power P by $|E| = \sqrt{2P\kappa/\hbar\omega_L}$, is given by,

$$\hat{H}_{\text{drive}} = i\hbar (Ee^{-i\omega_L t} \hat{a}^\dagger - E^* e^{i\omega_L t} \hat{a}). \quad (\text{B2})$$

The other two terms are obtained from the energy of the field inside the cavity $\hbar\omega_c(\hat{q})(\hat{a}^\dagger \hat{a} - \langle \hat{a}^\dagger \hat{a} \rangle)$, where $\hat{a}^\dagger(\hat{a})$ are the creation(annihilation) cavity photon operators. The mean value of cavity photons is subtracted in order to fix the equilibrium position in the presence of the classical radiation pressure at $q = 0$. If this position is at the maximum slope of the standing wave inside the cavity, a linear dependence $\omega_c(\hat{q}) = \omega_c + \xi_0 \hat{q}$ is obtained, where $\omega_c = \omega_c^0 + \delta$. The shift δ is caused by the equilibrium position of the dielectric object. See appendix D for the specific quantities considering spheres and rods. Next, in the displaced frame one can write $\hat{a} = \alpha + \hat{a}'$ (the prime will be omitted hereafter), where $|\alpha| = \sqrt{n_{\text{ph}}}$ is the square root of the number of cavity photons. Putting all together one has $\hat{H}_r = \hbar\omega_c \hat{a}^\dagger \hat{a}$ and

$$\hat{H}_{\text{OM}} = \hbar|\alpha|q_m\xi_0(\hat{b}^\dagger + \hat{b})(\hat{a}^\dagger + \hat{a}). \quad (\text{B3})$$

We neglected the coupling term which is not proportional to $\sqrt{n_{\text{ph}}}$, which is typically of the order of 10^5 . Therefore, one obtains then that the optomechanical coupling is $g = |\alpha|g_0$, with $g_0 = q_m\xi_0$. Note that the large term $|\alpha|$, compensates the small ground state size q_m .

APPENDIX C: SELF-TRAPPING USING TWO MODES

The self-trapping consists in using two optical modes $\hat{a}_{1(2)}$, and combine them so that they provide trapping as well as the optomechanical coupling. The initial Hamiltonian in this case would be

$$\hat{H} = \frac{\hat{p}_q^2}{2m} + \hbar\omega_{c,1}(q)\hat{a}_1^\dagger \hat{a}_1 + \hbar\omega_{c,2}(q)\hat{a}_2^\dagger \hat{a}_2 + H_L. \quad (\text{C1})$$

In the displaced frame, $\hat{a}_{1(2)} = \alpha_{1(2)} + \hat{a}'_{1(2)}$ (we omit the primer hereafter), where $|\alpha_{1(2)}|$ is the square root of the number of photons for the mode 1(2). Then, by expanding the resonance frequency up to the second order around $q = 0$, *i.e.* $\omega_{c,1(2)}(q) = \omega_{c,1(2)} + \omega'_{c,1(2)}q + \omega''_{c,1(2)}q^2/2$, fixing the key condition $|\alpha_1|^2\omega'_{c,1} = -|\alpha_2|^2\omega'_{c,2}$, and neglecting subdominant terms, one obtains the Hamiltonian

$$\hat{H} = \frac{\hat{p}_q^2}{2m} + \frac{m\omega_t^2}{2}\hat{q}^2 + \hbar \sum_{i=1}^2 \left[(\xi_i \hat{a}_i^\dagger \hat{q} + \text{H.c.}) + \omega_{c,i} \hat{a}_i^\dagger \hat{a}_i \right] + \hat{H}_L. \quad (\text{C2})$$

We have defined $\omega_t = [\hbar(\omega''_{c,1}|\alpha_1|^2 + \omega''_{c,2}|\alpha_2|^2)/m]^{1/2}$ and $\xi_i = \omega'_i\alpha_i$. Thus, provided $\omega''_{c,1}|\alpha_1|^2 + \omega''_{c,2}|\alpha_2|^2 > 0$, one has the desired self-trapping and optomechanical coupling with the help of the two modes.

APPENDIX D: OPTOMECHANICAL COUPLING AND TRAPPING

We compute here the optomechanical coupling for the sphere, assuming external trapping, and for the rod using self-trapping. In the latter, we derive two configurations required for cooling either the center-of-mass translational motion or the rotational motion.

1. Dielectric sphere

Let us consider the case of having a dielectric sphere of volume V and relative dielectric constant ϵ_r , and a TEM 00 mode in the cavity. Then, the dependence of the resonance frequency on the center-of-mass position $\vec{r} = (x, y, z)$, which can be obtained using (A1), is given by

$$\frac{\omega_c(\vec{r})}{\omega_c^0} \approx 1 - \frac{V(\epsilon_r - 1) [W^2 - 2(x^2 + y^2)] \cos^2(\omega_c^0 z/c)}{\pi W^4 d}. \quad (\text{D1})$$

Here W is the waist of laser at the center of the cavity, and d the cavity length. We consider a confocal cavity, $W = \sqrt{\lambda d/2\pi}$. The object is assumed to be placed close to the center of the cavity and that the radius of the sphere is smaller than the wavelength.

We suppose external trapping at $x_0 = y_0 = 0$ and $z_0 = c\pi/4\omega_c^0$, with frequency ω_t (D3). Then, the optomechanical coupling is given by $g_0 = \sqrt{\hbar/2\rho V \omega_t \xi_0}$, where $\xi_0 = \partial_z \omega_c(\vec{r})|_0$ can be computed using (D1), and reads

$$\xi_0 = \frac{(\omega_c^0)^2 (\epsilon_r - 1) V}{cd\pi W^2}. \quad (\text{D2})$$

The shifted frequency is $\omega_c = \omega_c(\vec{r}_0) = \omega_c^0 + \delta$, with $\delta = -V\omega_c^0(\epsilon_r - 1)/2d\pi W^2$.

The external trapping can be achieved by optical tweezers. For spheres of radius R , mass M , and relative dielectric constant ϵ_r , one can obtain, in the Rayleigh regime, that the trapping frequency is given by [19]

$$\omega_t^2 = \frac{6}{\rho c} \left(\frac{\epsilon_r - 1}{\epsilon_r + 2} \right) \frac{I_0}{W_0^2}, \quad (\text{D3})$$

where W_0 is the laser waist, and I_0 the field intensity.

2. Dielectric rod

When considering a rod, in order to simplify the calculation, we model it as two opposed ‘‘pieces of cake’’ of width a , arc L , and radius R , see Fig. 4. Note that this corresponds to a small section of the waist of the laser, since we will take $R = W/2$. The volume of the rod is

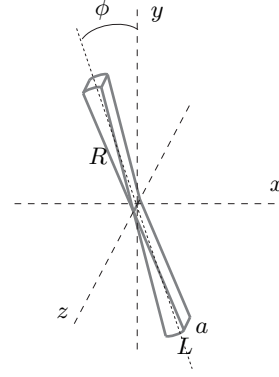


Fig. 4: The model used as a rod in order to simplify the calculations.

$V = RLa$, and its momentum of inertia $I = RLM/4\pi$, where M is its mass. In the case of having a counterrotating Laguerre-Gauss (LG) mode 10 and -10 , the frequency dependence on the rotational angle ϕ and center-of-mass z position (see Fig. 1c,d in the Letter) is given by

$$\frac{\omega_{c,1}(\phi, z)}{\omega_c^0} = 1 - \frac{V(\epsilon_r - 1) C_1 \cos^2[\omega_c^0 z/c] \cos^2[\phi]}{\pi W^2 d}, \quad (\text{D4})$$

with $C_1 = 2(2\sqrt{e} - 3)/\sqrt{e}$. In case of having a superposition of the LG modes 20 and -20 , one obtains the similar result

$$\frac{\omega_{c,2}(\phi, z)}{\omega_c^0} = 1 - \frac{V(\epsilon_r - 1) C_2 \cos^2[\omega_c^0 z/c] \cos^2[2\phi]}{\pi W^2 d}, \quad (\text{D5})$$

with $C_2 = (8\sqrt{e} - 13)/2\sqrt{e}$. The rod is assumed to be placed close to the center of the cavity and that its width a is much smaller than the cavity length.

We propose the self-trapping configuration (see appendix C) in order to trap both center-of-mass translation and rotation, using, as before, the superposition of LG modes 10 and -10 for the mode-1, and the superposition 20 and -20 for the mode-2.

In case of aiming at cooling the translational motion, the equilibrium position is obtained at $\phi_0 = 0$ and $z_0 = c\pi/8\omega_c^0$, by translating the mode-1 a distance $z_0 = c\pi/4\omega_c^0$ with respect to the mode-2. Then, using (D4) and (D5), one can compute the z -optomechanical coupling $g_0^z = \sqrt{\hbar/2\rho V \omega_{t,z} \xi_0^z}$, with $\xi_0^z = \partial_z \omega_{c,1}(\phi, z)|_0$, which reads

$$\xi_0^z = -\frac{(\omega_c^0)^2 C_1 (\epsilon_r - 1) V}{c\sqrt{2}d\pi W^2} \quad (\text{D6})$$

One also has that $g_0^\phi = 0$. The trapping frequency for the translation along the z -axis, $\omega_{t,z}$, and for the rotation $\omega_{t,\phi}$, can be computed using $\partial_{zz}^2 \omega_{c,1(2)}(\phi, z)|_0$, and $\partial_{\phi\phi}^2 \omega_{c,1(2)}(\phi, z)|_0$. The shifted frequency is $\omega_{c,1(2)} = \omega_{c,1(2)}(\phi_0, z_0) = \omega_c^0 + \delta_{1(2)}$, with $\delta_{1(2)} = -V\omega_c^0(\epsilon_r - 1)C_{1(2)} \cos^2(\pi/8)/d\pi W^2$.

In case of cooling the rotational motion, the equilibrium position is obtained at $\phi_0 = 7\pi/12$ and $z_0 = 0$ by rotating the mode-1 an angle $\pi/4$ with respect to the mode-2. Then, one can compute the ϕ -optomechanical coupling $g_0^\phi = \sqrt{\hbar/2I\omega_{t,\phi}}\xi_0^\phi = \partial_\phi\omega_{c,1}(\phi, z)|_0$, which reads

$$\xi_0^\phi = -\frac{\omega_c^0 C_1 \sqrt{3}(\epsilon_r - 1)V}{2d\pi W^2}. \quad (\text{D7})$$

Also, $g_0^z = 0$. The trapping frequencies can be computed as in the translational motion coupling, but at the equilibrium position used for rotational cooling. The shifted frequency is in this case $\omega_{c,1(2)} = \omega_{c,1(2)}(\phi_0, z_0) = \omega_c^0 + \delta_{1(2)}$, with $\delta_{1(2)} = -3V\omega_c^0(\epsilon_r - 1)C_{1(2)}/4d\pi W^2$.

Finally, let us mention that by a trapping provided externally, for instance, by means of optical tweezers, one could place the rod at the maximum slope of both the translational and azimuthal standing wave. Then, one would get $g_0^\phi \neq 0$ and $g_0^z \neq 0$ at the same time, and hence, one could cool both degrees of freedom simultaneously provided the trapping is tight enough.

APPENDIX E: HEATING AND DAMPING DUE TO GAS PRESSURE

Let us analyze here the heating and damping of the mechanical motion of the center-of-mass of a dielectric sphere due to the impact of air molecules inside the vacuum chamber. The air molecules of mass m have mean velocity $\bar{v} = \sqrt{3K_b T/m}$, where T is the temperature of the chamber, assumed to be at room temperature, and K_b is the Boltzmann's constant. The pressure inside the vacuum chamber is P , and the dielectric sphere has mass M , radius R , and is harmonically trap with frequency ω_t .

One can hence consider the Harmonic oscillator with additive white noise:

$$\ddot{z} + 2\gamma\dot{z} + \omega_t^2 z = \xi(t). \quad (\text{E1})$$

The stochastic force $\xi(t)$ describes the impact of air molecules. For white noise one has that $\langle \xi(t)\xi(t') \rangle = 2M^2 D \delta(t-t') = 4K_b T M \gamma \delta(t-t')$ (thus $D = 2K_b T \gamma / M$), where in the last equation we have used the fluctuation dissipation theorem. The variance of the position can be computed solving the differential stochastic equation and supposing $\omega \gg \gamma$ (always fulfilled in our levitating spheres) reads

$$\langle [z(t) - \langle z(t) \rangle]^2 \rangle \approx \frac{D}{2\gamma\omega^2} \{1 - e^{-2\gamma t}\}. \quad (\text{E2})$$

By considering the equipartition principle, the variance allows us to compute the increase of energy by taking $\Delta E(t) = M\omega^2 \langle [z(t) - \langle z(t) \rangle]^2 \rangle$. Hence one can compute the time t^* required to increment one quantum $\hbar\omega$ of energy in the quantum harmonic oscillator. This time

should be larger than the inverse of the laser cooling rate Γ , which is defined as the time required to decrease one quantum of energy. The time t^* is given by solving $\Delta E(t^*) = \hbar\omega$ and reads

$$t^* = -\frac{1}{2\gamma} \log \left(1 - \frac{\hbar\omega}{K_b T} \right) \approx \frac{\hbar\omega}{K_b T 2\gamma}, \quad (\text{E3})$$

where we have used $\hbar\omega \ll K_b T$. Then the condition for ground state cooling is given by

$$t^* \Gamma = \frac{\Gamma \hbar\omega}{K_b T 2\gamma} \gg 1. \quad (\text{E4})$$

We determine now an expression for γ which will depend on the properties of the gas surrounding the harmonic oscillator. We will derive it through kinetic theory. Assume our sphere is moving with velocity v . At the reference frame where the sphere has velocity equal to zero, one can compute the decrease of momentum of the sphere by the balance of momenta, given by the impact of one third of the particles colliding from behind with a velocity $\bar{v} - v$, minus those colliding in front with velocity $v + \bar{v}$. This can be written as

$$\begin{aligned} \frac{\Delta p}{\Delta t} &= (\bar{v} - v)\pi R^2 \frac{\rho}{3m} 2m(\bar{v} - v) - (\bar{v} + v)\pi R^2 \frac{\rho}{3m} 2m(\bar{v} + v) \\ &= -\frac{4\pi R^2 \rho \bar{v}}{3M} 2Mv = -\gamma 2Mv, \end{aligned} \quad (\text{E5})$$

Using that the pressure of the gas is related to the density by $\rho = 3P/\bar{v}^2$, one obtains that

$$\gamma = \frac{4\pi R^2 P}{M\bar{v}} \quad (\text{E6})$$

Thus, inserting the value of gamma in (E4), one finds an upper bound for the pressure required inside the vacuum chamber

$$P \ll \frac{3M\Gamma\hbar\omega}{8m\bar{v}\pi R^2} \sim \Gamma \times 10^{-12} \text{ Torr Hz}^{-1}. \quad (\text{E7})$$

We have used the spheres described in appendix H, and that the mass of molecules of air is $m \sim 28.6$ u and $T = 300\text{K}$. Recalling that the typical cooling rate is of the order of hundreds of kHz [13, 14, 15], one obtains the typical pressures of order 10^{-6} Torr used in experiments. With this pressure we have a damping of the order of mHz, which leads to extremely good mechanical quality factors of the order of 10^9 .

APPENDIX F: BULK TEMPERATURE

In order to estimate the bulk temperature of the dielectric object attained after being heated by the lasers, we assume it behaves as a blackbody. Then, the steady state of the dielectric objects fulfills that the power absorbed

$$P_{\text{abs}} = \frac{\omega L}{2} |E|^2 \Im[\alpha], \quad (\text{F1})$$

where ω_L is the laser frequency, E the electric field, and α the polarizability, equals the power dissipated P_{rad} through black-body radiation

$$P_{\text{rad}} = Ae\sigma [T^4 - T_{\text{env}}^4], \quad (\text{F2})$$

where A is the area of the object, e the emissivity (≈ 1), σ the Stefan-Boltzmann constant, T_{env} the temperature of the vacuum chamber, and T the bulk temperature. Thus, from $P_{\text{abs}} = P_{\text{rad}}$ one obtains the bulk temperature T . For a sphere of radius R trapped by optical tweezers, this corresponds to

$$T^4 = I_0 \frac{4\pi^3 R}{e\sigma\lambda} \frac{3\epsilon_2}{(\epsilon_1 + 2)^2 + \epsilon_2^2} + T_{\text{env}}^4 \quad (\text{F3})$$

where P is the laser power and $\epsilon_r = \epsilon_1 + i\epsilon_2$ the complex relative dielectric constant. Note that only here we have assumed ϵ_r to be complex, since ϵ_2 is generally very small for the objects we consider.

APPENDIX G: PROTOCOL TO CREATE QUANTUM SUPERPOSITION STATES

Let us derive here the protocol to create quantum superposition phononic states of the type (2). We use the quantum Langevin equations and the input-output formalism. After going to the rotating frame with the laser frequency ω_L , which is detuned to the resonance frequency by $\Delta = \omega_c - \omega_L$, displacing the photonic operators $\hat{a} = \alpha + \hat{a}'$ (we will omit the prime hereafter), choosing $\alpha = E/(i\Delta + \kappa)$, so that the constant terms cancel, and neglecting subdominant terms, one obtains the quantum Langevin equation for the total Hamiltonian \hat{H}_T (B1)

$$\begin{aligned} \dot{\hat{a}} &= -(i\Delta + \kappa)\hat{a} - ig(\hat{b}^\dagger + \hat{b}) + \sqrt{2\kappa}\hat{a}_{\text{in}}(t)e^{i\omega_L t}, \\ \dot{\hat{b}} &= -(i\omega_t + \gamma)\hat{b} - ig(\hat{a}^\dagger + \hat{a}) + \sqrt{2\gamma}\hat{b}_{\text{in}}(t). \end{aligned} \quad (\text{G1})$$

Note that one has the enhanced optomechanical coupling $g = |\alpha|g_0$. In the interaction picture, *i.e.* $\hat{a}_I = \hat{a}e^{i\Delta t}$ and $\hat{b}_I = \hat{b}e^{i\omega_t t}$, if one chooses $\Delta = \omega_t$ (red-sideband), and perform the rotating-wave-approximation (valid for $\omega_t \gg g$), derives the final equations

$$\begin{aligned} \dot{\hat{a}}_I &= -\kappa\hat{a}_I - ig\hat{b}_I + \sqrt{2\kappa}\hat{a}_{\text{in}}(t)e^{i(\omega_L + \Delta)t} \\ \dot{\hat{b}}_I &= -\gamma\hat{b}_I - ig\hat{a}_I + \sqrt{2\gamma}\hat{b}_{\text{in}}(t)e^{i\omega_t t}. \end{aligned} \quad (\text{G2})$$

Next, we consider that the input for the photonic state is a light pulse with gaussian shape centered at the resonance frequency ω_c , that is,

$$|\psi\rangle = \int d\omega \phi(\omega) \hat{a}_0^\dagger(\omega) |\Omega\rangle, \quad (\text{G3})$$

where $\hat{a}_0^\dagger(\omega)$ ($\hat{a}_0(\omega)$) are creation(annihilation) photonic operators out of the cavity at frequency ω , and $\phi(\omega)$ \propto

$\exp[-(\omega - \omega_c)^2/\sigma^2]$. Then, by recalling that $\hat{a}_{\text{in}}(t) = \int d\omega e^{-i\omega t} \hat{a}_0(\omega)/\sqrt{2\pi}$, one has that $\langle \psi | \hat{a}_{\text{in}}(t) | \psi \rangle = 0$ and $\langle \psi | \hat{a}_{\text{in}}^\dagger(t) \hat{a}_{\text{in}}(t') | \psi \rangle = \tilde{\phi}^*(t) \tilde{\phi}(t')$ (where $\tilde{\phi}(t)$ is the Fourier transform of $\phi(\omega)$). Solving the differential equations and obtaining $\hat{b}_I^\dagger(t)$, one can compute $\langle \hat{b}_I \rangle(t)$ (which is trivially zero since $\langle \hat{a}_{\text{in}}(t) \rangle = \langle \hat{b}_{\text{in}}(t) \rangle = 0$), and $\langle \hat{b}_I^\dagger \hat{b}_I \rangle(t)$. The quantity $\langle \hat{b}_I^\dagger \hat{b}_I \rangle(t)$ is plotted in Fig. 2b, for $g/\kappa = 1$ and $g/\kappa = 0.25$, with $\sigma = \kappa$ and $\gamma \sim 0$. For the ideal case, half of the one-photon pulse enters into the cavity and at some particular time t^* , the entangled state

$$|E\rangle_{ab} = \frac{1}{\sqrt{2}} (|\tilde{0}\rangle_a |1\rangle_b + |\tilde{1}\rangle_a |0\rangle_b), \quad (\text{G4})$$

is prepared. Here, $|\tilde{0}\rangle_a$ ($|\tilde{1}\rangle_a$) is the displaced vacuum (displaced one photon) state of the light system corresponding to the output field. This state yields $\langle \hat{b}_I(t^*) \rangle = 0$ and $\langle \hat{b}_I^\dagger(t^*) \hat{b}_I(t^*) \rangle = 1/2$ similarly to the result obtained in Fig. 2b. The protocol finishes by performing the balanced homodyne measurement of the quadrature $\hat{X}_L = (\hat{a}_{\text{out}}^\dagger + \hat{a}_{\text{out}})$ at time t^* . If one obtains the value x_L , the superposition state

$$|\Psi\rangle_b = \frac{1}{\sqrt{2}} (c_0|0\rangle_b + c_1|1\rangle_b), \quad (\text{G5})$$

is prepared, where $c_{0(1)} = \langle x_L | \tilde{1}(\tilde{0}) \rangle_a$. At the same time of the measurement, the driving field is switched off.

APPENDIX H: EXPERIMENTAL PARAMETERS FOR STRONG COUPLING AND GROUND STATE COOLING OF DIELECTRIC SPHERES AND RODS

We consider a confocal cavity of length $d = 4$ mm, with a resonant laser at $\lambda = 1064$ nm, which gives a waist at the center of the cavity of $W = \sqrt{\lambda d/2\pi} \approx 26.0$ μm . If we assume a high-finesse optical cavity with $\mathcal{F} = 10^5$, then the decaying rate is $\kappa = c\pi/2\mathcal{F}d = 2\pi \times 188$ kHz.

The dielectric objects are considered to be made of fused silica, with a density $\rho = 2201$ Kg/m³ and relative dielectric constant $\epsilon_r = 2.1$. We take spheres of radius 250 nm, and rods with length equal to the waist W , width $a = 50$ nm, and arc length $L = 50$ nm.

Using a laser of 1064 nm, and a ratio $I_0/W_0^2 = 2$ W/ μm^4 , one has that the trapping frequency of the center-of-mass translation for the dielectric sphere provided by the optical tweezers is $\omega_t = 2\pi \times 351$ kHz (see (D3)). Hence, $\kappa/\omega_t \sim 0.53$ places us well in the good cavity regime required for ground state cooling. On the other hand, the enhanced optomechanical coupling, with laser powers of 0.5 mW, gives $g = 2\pi \times 182$ kHz, which also places us in the strong coupling regime $g \gtrsim \kappa, \gamma$.

Regarding the dielectric rod, for the translational motion cooling scheme, we achieve trapping frequencies

of $\omega_{t,z} = 2\pi \times 552$ kHz, and $\omega_{t,\phi} = 2\pi \times 848$ kHz, and optomechanical coupling of $g_z = 2\pi \times 243$ kHz. For the rotational cooling, one has trapping frequencies $\omega_{t,z} = 2\pi \times 492$ kHz, $\omega_{t,\phi} = 2\pi \times 503$ kHz, and optomechanical coupling $g_\phi = 2\pi \times 276$ kHz. We assumed driving powers for the mode-1 of 4 mW. In both cases, one gets the good cavity and strong coupling regimes.

Optical grade fused silica presents a very low absorption at 1064 nm, with $\epsilon_1 = 2.1$ and $\epsilon_2 = 2.5 \times 10^{-10}$. In these experimental conditions, the bulk temperature achieved for the dielectric spheres is just around four degrees above the room temperature when using the optical tweezers.

-
- [1] Zoller, P., *et al.* Quantum information processing and communication. *Eur. Phys. J. D* **36**, 203–228 (2005).
- [2] Arndt, M., *et al.* Wave-particle duality of c60 molecules. *Nature* **401**, 680–682 (1999).
- [3] Deléglise, *et al.* Reconstruction of non-classical cavity field states with snapshots of their decoherence. *Nature* **455**, 510–514 (2008).
- [4] Hammerer, K., Sorensen, A. S., and Polzik, E. S. Quantum interface between light and atomic ensembles. Preprint at (<http://arxiv.org/abs/0807.3358>) (2008).
- [5] Friedman, J. R., Patel, V., Chen, W., Tolpygo, S. K., and Lukens, J. E. Quantum superposition of distinct macroscopic states. *Nature* **406**, 43–46 (2000).
- [6] Marshall, W., Simon, C., Penrose, R., and Bouwmeester, D. Towards quantum superposition of a mirror. *Phys. Rev. Lett.* **91**, 130401 (2003).
- [7] Kippenberg, T. and Vahala, K. Cavity optomechanics: Back-action at the mesoscale. *Science* **321**, 1172–1176 (2008).
- [8] Marquardt, F. and Girvin, S. Optomechanics. *Physics* **2**, 40 (2009).
- [9] Favero, I. and Karrai, K. Optomechanics of deformable optical cavities. *Nature Photon.* **3**, 201–205 (2009).
- [10] Rothschild, L. J. and Mancinelli, R. L. Life in extreme environments. *Nature* **406**, 1092–1101 (2001).
- [11] Ashkin, A. and Dziedzic, J. M. Optical trapping and manipulation of viruses and bacteria. *Science* **235**, 1517–1520 (1987).
- [12] Schrödinger, E. Die gegenwärtige situation in der quantenmechanik. *Naturwissenschaften* **23**, 807–812,–823–828, 844–849 (1935).
- [13] Wilson-Rae, I., Nooshi, N., Zwerger, W., and Kippenberg, T. J. Theory of ground state cooling of a mechanical oscillator using dynamical backaction. *Phys. Rev. Lett.* **99**, 093901 (2007).
- [14] Marquardt, F., Chen, J. P., Clerk, A. A., and Girvin, S. M. Quantum theory of cavity-assisted sideband cooling of mechanical motion. *Phys. Rev. Lett.* **99**, 093902 (2007).
- [15] Genes, C., Vitali D., Tombesi P., Gigan S., and Aspelmeyer M. Ground-state cooling of a micromechanical oscillator: Comparing cold damping and cavity-assisted cooling schemes. *Phys. Rev. A* **77**, 033804 (2008).
- [16] Groeblacher, S., *et al.* Demonstration of an ultracold micro-optomechanical oscillator in a cryogenic cavity. *Nature Phys.* **5**, 485–488 (2009).
- [17] Thompson, J. D., *et al.* Strong dispersive coupling of a high-finesse cavity to a micromechanical membrane. *Nature* **452**(7183), 72–75 (2008).
- [18] Schliesser, A., Rivière, R., Anetsberger, G., Arcizet, O., and Kippenberg, T. J. Resolved-sideband cooling of a micromechanical oscillator. *Nature Phys.* **4**, 415–419 (2008).
- [19] Ashkin, A., Dziedzic, J. M., Bjorkholm, J. E., and Chu, S. Observation of a single-beam gradient force optical trap for dielectric particles. *Opt. Lett.* **11**, 288–290 (1986).
- [20] Groeblacher, S., Hammerer, K., Vanner, M. R., and Aspelmeyer, M. Observation of strong coupling between a micromechanical resonator and an optical cavity field. *Nature* **460**, 724–727 (2009).
- [21] Bhattacharya, M. and Meystre, P. Using a Laguerre-Gaussian beam to trap and cool the rotational motion of a mirror. *Phys. Rev. Lett.* **99**, 153603 (2007).
- [22] Lvovsky, A. I., *et al.* Quantum state reconstruction of the single-photon fock state. *Phys. Rev. Lett.* **87**, 050402 (2001).
- [23] Duan, L. M. and Kimble, J. H. Scalable Photonic Quantum Computation through Cavity-Assisted Interactions. *Phys. Rev. Lett.* **92**, 127902 (2004).
- [24] Ourjoumtsev A., Jeong H., Tualle-Broui R., and Grangier P. Generation of optical “Schrödinger cats” from photon number states. *Nature* **448**, 784–786 (2007).
- [25] Greiff, D. and Rightsel, W. A. Stabilities of dried suspensions of influenza virus sealed in a vacuum of under different gases. *Appl. Microbiol.* **17**, 830–835 (1969).
- [26] Steckl, A. J. DNA - A new material for photonics?. *Nature Photon.* **1**, 3–5 (2007).
- [27] Nelson, D. R. Current status of the tardigrada: Evolution and ecology. *Int. Comp. Biol.* **42**, 652–659 (2002).
- [28] Jönsson, K. I., Rabbow, E., Schill, R. O., Harms-Ringdahl, M., and Rettberg, P. Tardigrades survive exposure to space in low earth orbit. *Curr. Biol.* **17**, R529–R531 (2008).
- [29] Simon, C. Conscious observers clarify many worlds. Preprint at (<http://arxiv.org/abs/0908.0322>) (2009).